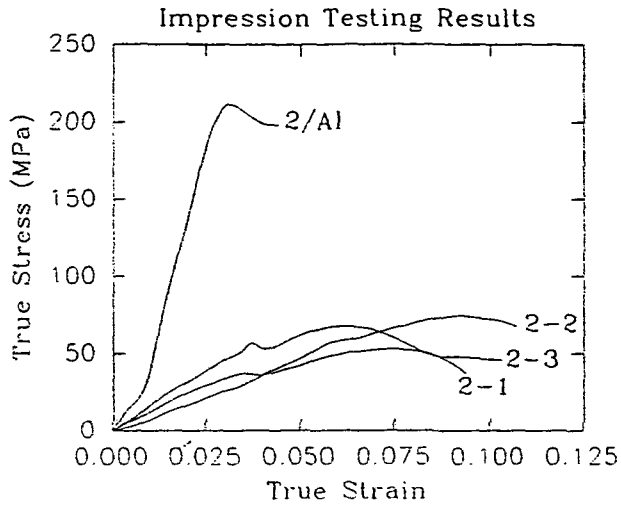

Fig. 1. Results of impression tests. 2-1, 2-2, and 2-3 are samples from experiment 13B917 without binder. 2/Al is from experiment 14B917 with aluminum binder.

There are two noteworthy features that are evident from optical microscopy:

1. Compact densities are strongly influenced by the addition of aluminum particles. The metal appears to have acted as a lubricant to enhance densification through interparticle sliding and rotation.

2. Aluminum particles are well dispersed as thin boundary layers between simulant particles. This type of mixing cannot be easily achieved by conventional mixing methods. Also, thinly dispersed layers may be exploited to enhance postshock processing of shock-compacted materials by acting as an agent for dynamic reaction sintering of lunar materials.

Impression Testing: Stress vs. strain curves were determined with a WC indentor (diameter = 1 mm, cross-head speed = 0.002 in/min). Material recovered from experiment 13B917 (no binder) was sampled from three different locations (2-1, 2-2, and 2-3). One sample (2/Al) was taken from experiment 14B917 (Al binder). Stress-strain data for these four samples are summarized in Table 1, and plotted in Fig. 1. The following is a brief summary of impression testing results for the two recovery experiments.

13B917 (no binder): Samples 2-2 and 2-3 yielded nearly identical values for strengths, but the strains were not consistent. When the samples were crushed, there was not enough strain energy to cause them to fly.

14B917 (Al binder): Sample 2/Al was much stronger (see Fig. 1). Moreover, the failure mode was quite different from the other samples. The resistance to impression was very large, higher by a factor of about 3. The elastic modulus was higher by a factor of about 6. Strain energy caused the sample to shatter under maximum load, launching fragments at high velocity.

This work was supported by the U.S. Dept. of Energy under contract DE-AC0476DP00789.

References: [1] Murr L. E. et al. (1986) *Metallurgical Applications of Shock-Wave and High-Strain-Rate Phenomena*, Marcel Dekker, New York, 1120 pp. [2] Graham R. A. and Sawaoka A. B., *High Pressure Explosive Processing of Ceramics*, Trans. Tech., Switzerland, 404 pp. [3] Graham R. A. and Webb D. M. (1984) In *Shock Waves in Condensed Matter—1983* (J. R. Asay et al., eds.), 423–424, North Holland, Amsterdam. [4] Graham R. A. and Webb D. M. (1986) In *Shock Waves in Condensed Matter* (Y. M. Gupta, ed.), 719–724, Plenum, New York. [5] Weiblen P. W. et al. (1990) In *Proceedings of Space 90*, 98–106, ASCE.

N93-17239 1993008050 487777

A LUNAR PENETRATOR TO DETERMINE SOLAR-WIND-IMPLANTED RESOURCES AT DEPTH IN THE LUNAR REGOLITH. W. Boynton[1], W. Feldman[2], and T. Swindle[1], [1]University of Arizona, Tucson AZ 85718, USA, [2]Los Alamos National Laboratory, Los Alamos NM 87454, USA.

Introduction: Several volatiles implanted into the lunar regolith by the solar wind are potentially important lunar resources. *^{3}He might be mined as a fuel for lunar nuclear fusion reactors* [1]. Even if the mining of ^{3}He turns out not to be feasible, several other elements commonly implanted by the solar wind (H, C, and N) could be important for life support and for propellant or fuel production for lunar bases [2]. We propose a simple penetrator-borne instrument package to measure the abundance of H at depth. Since solar-wind-implanted volatiles tend to correlate with one another, this can be used to estimate global inventories and to design extraction strategies for all of these species.

Current Knowledge: A considerable amount is known about the distribution of solar-wind-implanted volatiles from analyses of Apollo and Luna samples. Since the energy of the solar wind is only sufficient to implant ions to depths of less than a micrometer into grains, these volatiles are only found on grain surfaces that were once exposed to the solar wind. However, the regolith is constantly gardened by impacts, so volatiles are mixed to depths of order several meters. Models predict that the hydrogen abundance of formerly exposed grains will fall off with depth in the lunar regolith (e.g., the model of [3] predicts an exponential fall-off with an e-folding distance of about 3 m). The Apollo drill cores are not much help in testing this because their lengths are short compared to the scales of interest (only one is longer than 2 m, and that one is only 3 m). In fact, the Apollo cores do not clearly show that there is any systematic decrease in volatile abundance with depth for the first 2–3 m [4]. This uncertainty could have a large impact on resource evaluation [4]: assuming that volatiles are uniformly distributed throughout the regolith (8–15 m deep) leads to a factor of 10 higher estimated global inventory than does assuming the distribution derived from the model of [3]. Furthermore, mining strategies for a resource found throughout the top 10 m or so of the regolith might be substantially different from ones for a resource found only in the top 2 or 3 m.

In the Apollo samples, most of the solar-wind-implanted volatiles correlate with one another and with other measures of soil "maturity" (extent of exposure to the solar wind) [5]. The exceptions are He and Ne, whose abundances show a strong dependence on the amount of the mineral ilmenite (and hence the Ti content). However, He and Ne also correlate with maturity if the Ti abundance is factored out [6]. Although the correlation of H content with maturity is not as strong as for some other elements in the Apollo samples (perhaps reflecting the difficulty in eliminating H contamination of the dry lunar soils), measurements of H with depth in the regolith should be indicative of all solar-wind-implanted species.

Basis of the Technique: Simple neutron counters have been shown to provide high sensitivity for the detection of low H

concentrations from orbit under the assumption of an infinitely deep homogeneous chemistry, when the major-element composition is simultaneously determined using a gamma ray detector [7,8]. Newer calculations reported here show that interpretation of these data can be in error if the hydrogen content of the near-surface regolith is not homogeneous.

Hydrogen is notable for its high efficiency in moderating cosmic-ray-induced fast neutrons to thermal energies. The ratio of thermal to epithermal neutrons (those in the process of slowing) is a very strong function of the hydrogen content. In order to get high precision at low H concentration, however, the abundances of elements that strongly absorb thermal neutrons such as, e.g., Ti, Fe, Sm, and Gd, also need to be determined.

Recent calculations [7,8] showed that a determination of the hydrogen content down to levels of 10 ppm from orbit requires only a 1% statistical precision. However, interpretation of these data is subject to systematic uncertainties that may be larger than the 1% level, depending on the nature and magnitude of H abundance variations as a function of depth. Basically, the reduced mean-scattering path of thermal neutrons caused by the presence of H tends to concentrate neutrons from surrounding material into the high-hydrogen-content side of abundance-changing interfaces. For example, comparison of a lunar meteoritic chemistry loaded uniformly with 100 ppm of hydrogen down to 200 g/cm^2 below the surface, and then with 10 ppm H to the 900 g/cm^2 level, with the same chemistry loaded with 100 or 10 ppm H uniformly down to the 900 g/cm^2 level, shows about 2% variation in subsurface gamma ray production rates (and hence in thermal neutron number density).

Instrumentation: The neutron detection is made with two identical ^{3}He gas proportional counters, one being bare and the other being wrapped in Cd. The bare detector is sensitive to both thermal and epithermal neutrons, whereas the one wrapped in Cd is sensitive only to epithermal neutrons because Cd is a strong absorber of thermal neutrons. The abundances of the strong neutron absorbers in the soil will be made with a simple scintillator gamma ray spectrometer. Although this type of detector does not offer the high sensitivity of cooled semiconductor detectors, they are more than adequate for determination of the abundances of Fe and Ti, the principal neutron absorbers on the Moon. Samarium and Gd are not easily detected with this approach, but because of our extensive database of lunar rock types, these elements can be estimated easily from the abundances of other elements that will be determined with the GRS, especially K, U, and Th.

Delivery and Support System: The instruments will be delivered to the lunar surface via a penetrator with a separable afterbody. Using the soil penetration equations of [9] and assuming a penetrability comparable to dry silt or clay, a forebody mass of 30 kg, a diameter of 7.5 cm, and an impact velocity of 100 m/s, the forebody will penetrate to a depth of about 10 m while the afterbody will remain partially exposed on the surface to maintain communication with Earth. Reduction in this maximum depth can be readily achieved by reducing the impact speed. Both parts will contain neutron and gamma detectors in order to compare the differences between the surface and deep abundances. The penetrator will be battery operated to provide a life of about one week on the lunar surface.

Conclusions: Calculations of the depth dependence of thermal, epithermal, and fast neutron fluxes and consequent capture gamma ray production rates have shown their utility in determining the depth profile of H at the 10 to 100 ppm sensitivity level. Orbital surveys of these same data are not capable of such a determination. The two techniques therefore complement one another. Whereas orbital surveys can provide comprehensive maps of suspected hydrogen concentrations due to solar wind implantation, a penetrator can provide ground truth for a small selection of sites to allow estimates of the depth dependence of such deposits and consequently an evaluation of the utility of such deposits as a source of resources to support human habitation on the Moon.

References: [1] Wittenburg et al. (1986) *Fusion Tech.*, *10*, 167. [2] Haskin (1989) *LPSC XX*, 387. [3] Arnold (1975) *Proc. LSC 6th*, 2375. [4] Swindle et al. (1990) *Mining Lunar Soils for ^{3}He*, UA/NASA SERC, Tucson. [5] Morris (1976) *Proc. LSC 7th*, 315. [6] Jordan (1990) In *Space Mining and Manufacturing, VII-38*, UA/NASA SERC, Tucson. [7] Metzger A. E. and Drake D. M. (1991) *JGR*, *96*, 449–460. [8] Feldman W. C. et al., *GRL*, *18*, 2157–2160. [9] Young C. W. (1972) *Sandia Lab. Rep. SC-DR-72-0523*.

N93-17240 1993008051 487979

ESTIMATING LUNAR PYROCLASTIC DEPOSIT DEPTH FROM IMAGING RADAR DATA: APPLICATIONS TO LUNAR RESOURCE ASSESSMENT.

B. A. Campbell[1], N. J. Stacy[2], D. B. Campbell[2], S. H. Zisk[1], T. W. Thompson[3], and B. R. Hawke[1], [1]Planetary Geosciences, SOEST, University of Hawaii, Honolulu HI, USA, [2]NAIC, Cornell University, Ithaca NY, USA, [3]Jet Propulsion Laboratory, California Institute of Technology, Pasadena CA, USA.

Introduction: Lunar pyroclastic deposits represent one of the primary anticipated sources of raw materials for future human settlements [1]. These deposits are fine-grained volcanic debris layers produced by explosive volcanism contemporaneous with the early stages of mare infilling [2,3]. There are several large regional pyroclastic units on the Moon (for example, the Aristarchus Plateau, Rima Bode, and Sulpicius Gallus formations), and numerous localized examples, which often occur as dark-halo deposits around endogenic craters (such as in the floor of Alphonsus Crater). Several regional pyroclastic deposits have been studied with spectral reflectance techniques: The Aristarchus Plateau materials were found to be a relatively homogeneous blanket of iron-rich glasses [4,5]. One such deposit was sampled at the Apollo 17 landing site, and was found to have ferrous oxide and titanium dioxide contents of 12% and 5% respectively [6]. While the areal extent of these deposits is relatively well defined from orbital photographs, their depths have been constrained only by a few studies of partially filled impact craters and by imaging radar data [7,1]. In this work, we present a model for radar backscatter from mantled units applicable to both 70-cm and 12.6-cm wavelength radar data. Depth estimates from such radar observations may be useful in planning future utilization of lunar pyroclastic deposits.

Radar Scattering Model: The depth of a pyroclastic layer is estimated based upon the ratio of backscattered power between a mantled region and an area of unmantled terrain assumed to represent the buried substrate. Several conditions are required: (1) Only the depolarized (same-sense circular) echo is modeled, to avoid consideration of large single-scattering facets; (2) there is no volume scattering within the pyroclastic (i.e., there are no inclusions large with respect to the radar wavelength); and (3) the depolarized backscatter originates largely within the regolith substrate, and not at its upper surface. Conditions (2) and (3) are supported by previous studies of the eclipse temperatures